PHILOSOPHICAL TRANSACTIONS OF THE ROYAL SOCIETY A MATHEMATICAL, PHYSICAL & ENGINEERING SCIENCES

Tensile First Cracking Strain and Strength of Hybrid Composites and Laminates

J. Aveston and A. Kelly

Phil. Trans. R. Soc. Lond. A 1980 **294**, 519-534
doi: 10.1098/rsta.1980.0061

Phil. Trans. R. Soc. Lond. A **294**, 519–534 (1980)
Printed in Great Britain

Tensile first cracking strain and strength of hybrid composites and laminates

J. Aveston† and A. Kelly, F.R.S.‡
† *National Physical Laboratory, Teddington, Middlesex, U.K.*
‡ *University of Surrey, Guildford, Surrey, U.K.*

[Plate 1]

A hybrid like a multidirectional laminate contains at least two major load-bearing components whose failure strains are different. The failure strain of the higher elongation component is invariably reduced by the presence of the other, but the ultimate strain of the lower elongation component may remain the same or can be increased by decreasing its dimensions. The relevant dimension may be the diameter of a bundle or of separate fibres or the thickness of the transverse ply in a 0°/90° laminate.

Our previous theory of multiple cracking and constrained failure is reviewed and applied to simple laminates and laminated hybrids. We also demonstrate that it can be applied to preventing cracking due to thermal strain. It is pointed out that, in 0°/90°/0° laminates, longitudinal splitting of the 0° plies may occur owing to the constraint imposed by the 90° plies, whether these have cracked or not.

Simple rules are given to account for the longitudinal ultimate strength and ultimate fracture strain of intermingled glass and carbon hybrids in epoxy resin. In this system, stress concentrations due to failure of the low elongation component do not appear to be very important.

1. Introduction

An increasing number of fibrous composites are being made that contain two types of fibre, and scientific studies of these are appearing in the literature (see, for example Kalnin 1972; Bunsell & Harris 1974; Lovell 1974; Hancox & Wells 1974; Walton & Majumdar 1975; Harris & Bradley 1976; Harris & Bunsell 1975; Aveston & Sillwood 1976; Paton 1977; Bradley & Harris 1977; Bader & Manders 1978). The two types of fibre may be either closely woven together and infiltrated with matrix simultaneously so that the composite consists of the two types closely intermingled, or else the composite may be made by bonding together separate lamellae each containing just one type of fibre in a resin. We shall call the two types *intermingled* or *interlaminated* respectively. They are illustrated in figure 1. In figure 1(*a*) and (*b*) the two types of fibre are shown as arranged parallel to one another, whereas in figure 1(*c*) it is recognized that the composite is a laminate with the separate lamellae containing different fibres each aligned in different directions.

The intermingled type of hybrid contains a relatively homogeneous distribution of fibres of the two types and its average mechanical properties can be described. It is usually made in order to achieve a cost of production intermediate between that of the two fibres and to improve the properties achievable by one type (usually the cheaper, e.g. glass), such as average stiffness and properties in fatigue, or else to improve the resistance to impact of a composite made solely of stiff, more brittle and more expensive fibres such as carbon (see for example A. W. Thompson, this volume).

The interlaminated composite is made usually with a specific structure in mind such as a hull structure, roof enclosure or pipe, i.e. in application to a plate or shell where the expensive stiffer fibre is located near a surface so as to increase the stiffness of the structure (Paton 1977).

The structural stiffness of a component made with an interlaminated hybrid construction can usually be adequately accounted for in terms of the elastic properties of the individual lamellae and their geometric distribution by using conventional plate and shell theory (Lekhnitskii 1968). The elastic properties of the individual lamellae containing just one type of fibre are measured, and it is not necessary to consider in detail how to relate the five independent elastic constants of an individual lamella to the properties and volume fractions of the fibre and resin within it. However, the explanation of the failure stresses of such structures is by no means so clear (see, for example, Paton 1977).

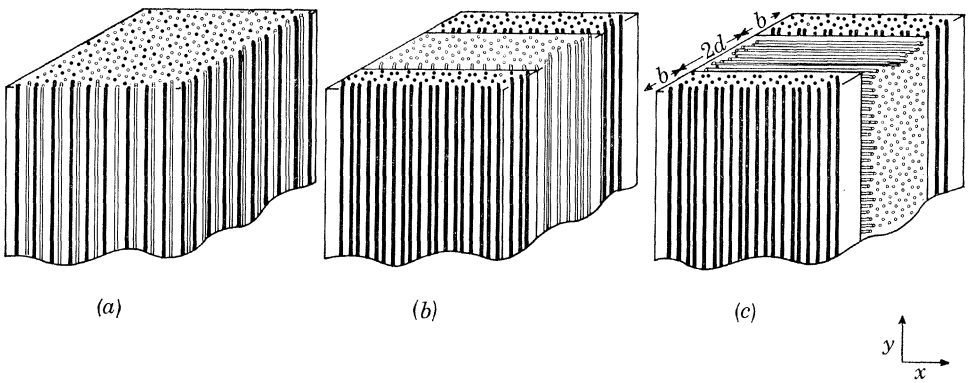

FIGURE 1. Hybrid fibre composites, (*a*), intermingled; (*b*), (*c*), interlaminated.

There are formulae available for the bounds on the elastic moduli of aligned fibrous composites containing fibres of a single kind (see, for example, Sendeckyj 1974 for a review). We are not aware of formulae available for application to fibrous composites consisting of two or more types of fibre.

The most comprehensive attempt to account for the failure load in tension of aligned fibrous composites containing just one type of fibre is due to Rosen and Zweben and colleagues (see, for example, Zweben 1972), and Zweben (1977) has applied the same ideas to the fracture of an intermingled hybrid composite. We consider these ideas in passing in § 2.5 below.

In this paper we want to draw a very clear distinction between the first appearance of cracks when a hybrid composite is strained and the strain (or stress) at which final failure occurs. Since we shall be dealing many times with components (phases) – matrix or fibre with different elongations to failure in tension – we shall refer to these in a particular composite as l.e. (lower elongation) and h.e. (higher elongation).

2. MULTIPLE FRACTURE

When loaded in flexure or in tension most types of fibre composite show a load–elongation curve of the type shown in figure 2. The initial stage of the curve is essentially elastic, and if the composite is unloaded in this region there is little or no residual strain. At the point marked 1 in figure 2 on all types of curve some cracking occurs. This may be breaking of one population of fibres in a hybrid – curve 2 (*a*) (flexure) and 2 (*c*) (tension), cracking in the 90° plies of a 0°/90°/0°

laminate (curve 2(*d*)) or cracking of the matrix in a composite consisting of aligned fibres in a very brittle matrix (curve 2(*b*)). Many other examples can be given. That cracking occurs has been adequately proved by both direct examination and acoustic emission. We shall identify the point 1 by the strain at which it first occurs and call it the first cracking strain. It is sometimes referred to as the limit of proportionality. Two most important experimental facts must be recognized at the outset and these are that if the strain corresponding to 1 is exceeded, then gross fatigue damage occurs in any cyclic test (Owen 1974) and that *in general* the strain at which first cracking occurs is size-dependent. By size-dependent we do not mean that it depends on the overall size of the specimen (though it may do so) but that it depends on the interfacial area available for transfer of stress between the two components, and hence for a given volume loading

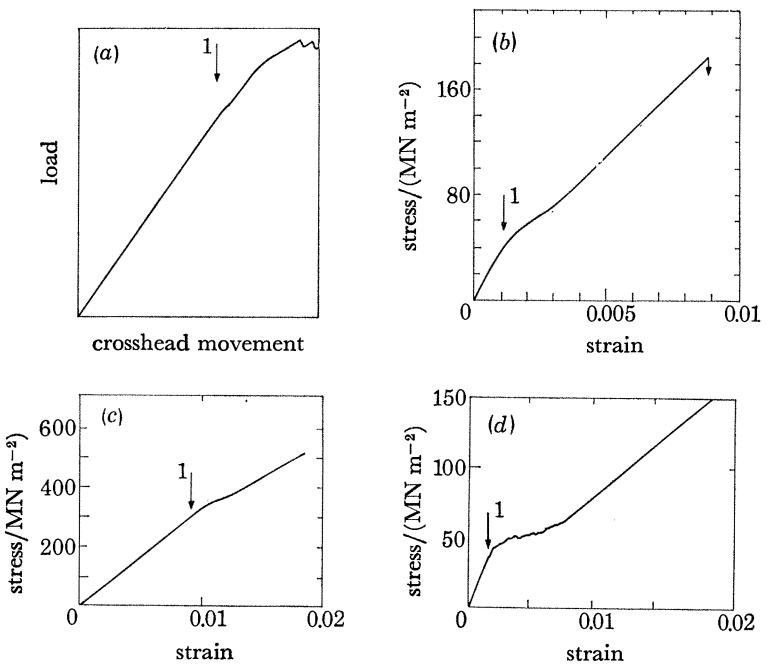

FIGURE 2. Stress–strain diagrams for composites undergoing multiple fracture. The point marked 1 indicates fracture of: (*a*) carbon in hybrid carbon–glass–epoxy beam in flexure (Hancox & Wells 1974); (*b*) cement in a carbon fibre reinforced cement (Aveston *et al.* 1974); (*c*) carbon in carbon–glass–epoxy hybrid (Aveston & Sillwood 1976); (*d*) 90° glass ply in glass–epoxy crossply laminate (specimen shown in figure 4).

on the size (frequently the diameter) of the dispersed component. For the examples given, in figure 2(*b*) and (*c*), it depends on the effective diameter of the tows of carbon fibre and in 2(*d*) on the thickness of the 90° lamellae.†

All of these effects may be predicted and discussed in terms of the theory of multiple cracking and constrained failure (Aveston *et al.* 1971; Aveston & Kelly 1973; Kelly 1974, 1976, 1978; Aveston & Sillwood 1976) in its various forms, some of which have been given less generally by other workers (Romualdi & Batson 1963; Argon & Shack 1975; Garrett & Bailey 1977*b*; see, also,

† Clearly in a bi-component composite with a given volume fraction of one component decreasing the size of the pieces of one component automatically means decreasing the size of the other, since pieces of one component separate the pieces of the other. When fibres are aligned in a matrix the separation of the surfaces of the fibre are on average given by s, which can be written in terms of the fibre diameter, d, as:

$$s = d[(\beta/V_1)^{\frac{1}{2}} - 1]$$

for a volume fraction V_1. The symbol β denotes a constant equal to 0.912 for a hexagonal array and to 0.785 for a square array. Clearly s and d vary in direct proportion. Decreasing the diameter of the fibres also decreases the spacing and one may speak of an effect depending on either fibre size or of fibre spacing interchangeably.

Tardiff 1973). We discuss this below with particular reference to hybrids, but since it is concerned with any fibrous composite in which one component fails while the other continues to bear the load, it has application to the control of cracking in a laminate consisting of plies of different orientation and so these are also considered in this paper.

2.1. *First cracking strain*

Multiple fracture is of very widespread occurrence, and occurs in situations as diverse as the cracking of a brittle lacquer on a ductile metal (Durelli & Okubo 1953) and the cracking of carbide whiskers in a high temperature eutectic (Bibring *et al.* 1972). It arises whenever one component in a multi-component system breaks at a smaller strain than the other *and* there is sufficient of the high elongation component to bear the total load at the first cracking strain. This condition is:

$$V_h \geqslant \frac{\sigma_{lu}}{\sigma_{hu} + \sigma_{lu} - \sigma'_h}, \tag{1}$$

or, in terms of strain, if the components are both elastic up to the first cracking strain, ϵ_{lu}, then:

$$\epsilon_{hu} \geqslant \epsilon_{lu}(1+\alpha), \tag{2}$$

where σ_u is the failure stress, ϵ_u the failure strain, σ'_h the stress on the h.e. component at failure of the l.e. component and h, l and c refer to the h.e. component, l.e. component and composite respectively with $\alpha = (E_l V_l / E_h V_h)$. It should be noted that it is assumed in this simple argument that there is no concentration of stress on the high elongation component when the component of lower elongation breaks.

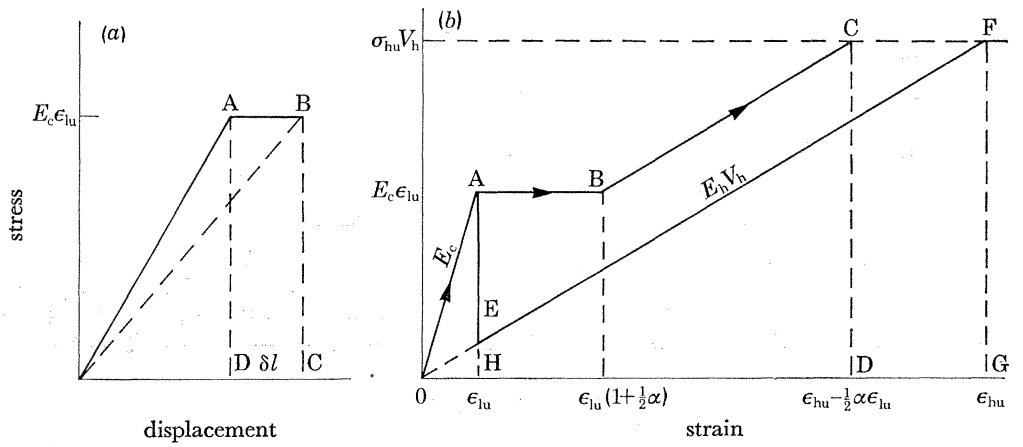

FIGURE 3. (*a*) Extension under *constant load* resulting from first transverse crack. Work available for formation of crack surfaces is $\frac{1}{2}E_c\epsilon_{lu}\delta l$. (*b*) Idealized stress–strain curve for specimen undergoing multiple cracking with crack spacing at the theoretical upper limit of $2x$ for a specimen with a single value of the cracking strain of the low elongation component (ϵ_{lu}).

If (1) is obeyed and the composite is strained above ϵ_{lu} then a series of parallel cracks appears in the l.e. phase. The spacing of these and their opening depends on the absolute scale of size of the microstructure, i.e. on the dimensions of one or of both components. Actual expressions for the spacing of the cracks, for the separation of the faces of the crack and for the cracking strain, depend on whether the two components remain elastically bound to one another after the initial cracking, which in turn depends on the maximum interfacial shear stress at the crack τ_{max} and

on the strength of the bond between the two components. However, in either case the formation of a single crack results in relaxation of the broken component on either side of the crack and hence an extension δl of the specimen (figure 3 (*a*)) due to the additional load borne by the h.e. component over a short distance on each side of the crack. For a frictional bond this transfer length depends on the limiting bond strength τ, and for the elastic case where the bond remains intact, on the shear modulus, but the important point to note, in either case, is that as the dispersion is increased (thinner fibres or lamellae of the l.e. phase) the rate of load transfer from the component bridging the crack is increased because the area of interface between the two components per unit volume is increased. Hence the length additionally strained of this component and hence the displacement of the ends of the specimen δl is decreased. As the product of the cracking stress $E_c \epsilon_{1u}$ and the displacement δl sets an *upper limit* to the work available from the loading system to form the crack, then if the surface work of fracture γ remains constant and δl is decreased, as a result of increased dispersion of the fibres or lamellae, a point is reached where ϵ_{1u} must increase above the value observed outside the composite before the required work of fracture can be extracted from the system. On the macroscale, consideration of the idealized stress–strain curve *OABC* (figure 3 (*b*)) leads to the same conclusion; the additional strain *AB* as a result of multiple cracking, and hence the work available, depends only α multiplied by the initial cracking strain, but the total number of cracks, and hence the energy required to form them, depends on the degree of dispersion, being greater for a greater dispersion.

In table 1 we collect the various formulae which will apply to the geometries in figure 1. The detailed derivations are in the references or can be obtained simply from them; e.g. for the plates (elastic case) the derivation follows that for the fibres (Aveston & Kelly 1973), except that the second term in equation 8*a* in that paper is zero and the boundary conditions are evaluated for a plate. The symbols not already defined are x, the minimum crack spacing ($2x$ is the maximum), b, the thickness of the h.e. plate, $2d$, the thickness of the l.e. plate, $2R$, the spacing between fibre centres and subscripts f and m, which refer to fibre and matrix. The term 2γ denotes the total fracture surface work of the phase which cracks. The term $\Delta\sigma_0$ is the maximum additional stress thrown onto the h.e. phase as a result of the cracks in the l.e. phase – i.e. it is the difference between the stress in the h.e. phase where it bridges the crack σ_a/V_h and the corresponding stress at a cross section where there is no crack, i.e. $\sigma_a E_h/E_c$ where σ_a is the applied stress. Thus

$$\Delta\sigma_0 = \left\{\frac{\sigma_a}{V_h} - \frac{\sigma_a E_h}{E_c}\right\}. \tag{3}$$

The formulae can be written in terms of the dimensions of either the h.e. or l.e. phase but when fibres are used either as an h.e. or l.e. phase it is easiest to write the formulae in terms of their dimensions (usually the diameter) since this is most easily controlled.

As expected, there is a close analogy between fibres and plates (r replaces b) and the frictional and elastic case (τ replaces τ_{max}) and a large measure of symmetry between multiple cracking of the fibres and matrix, but for the elastic case the symmetry is not complete because stress transfer is assumed to be through shear of the matrix in each case. Whether the elastic or frictional case applies depends on the value of τ_{max} which in turn depends largely on $\Delta\sigma_0$ and G_m. For example in fibre reinforced cement (high G, low V_f and high $\Delta\sigma_0$) the fibres will invariably debond when the matrix cracks (Aveston & Kelly 1973) whereas in laminates (low G, low $\Delta\sigma_0$) the bond is predicted to remain intact in the early stages of cracking and this is in fact observed (Parvizi *et al.* 1978). For instance, when initial cracking occurs, τ_{max} from equation (6) of this paper is equal

PHILOSOPHICAL TRANSACTIONS OF THE ROYAL SOCIETY A MATHEMATICAL, PHYSICAL & ENGINEERING SCIENCES

TABLE 1

component cracking first	geometry	bond type	x	ϵ_u^3	maximum shear stress	reference
matrix	aligned fibres	sliding friction	$\frac{\epsilon_{mu}E_f\alpha r}{2\tau}$ (1a)	$\frac{12\gamma_m V_m \tau}{E_c E_f \alpha^2 r}$ (1b)	τ found from experiment	Aveston *et al.* (1971); Spurrier & Luxmore (1976)
matrix	aligned fibres	elastic	$\frac{\epsilon_{mu}E_f\alpha r}{2\tau_{max}}$ (2a)	$\frac{4\gamma_m V_m \tau_{max}}{E_c\alpha^2 E_f r}$ (2b)	$\frac{\Delta\sigma_0}{2}\left[\frac{2G_m E_c}{E_f E_m V_m \ln(R/r)}\right]$ (2c)	Aveston & Kelly (1973)
fibres	aligned fibres	friction	$\frac{\epsilon_{fu}E_f\tau}{2\tau}$ (3a)	$\frac{12\gamma_f V_f \alpha^2 \tau}{E_c E_m r}$ (3b)	τ found from experiment	Aveston *et al.* (1971)
fibres	aligned fibres	elastic	$\frac{\epsilon_{fu}E_f\tau}{2\tau_{max}}$ (4a)	$\frac{4\gamma_f V_f \alpha^2 \tau_{max}}{E_c E_m V_m r}$ (4b)	$\frac{V_m}{V_f}\frac{\Delta\sigma_0}{2}\left[\frac{G_m}{E_f}\frac{V_f^{\frac{1}{2}}}{1-V_f^{\frac{1}{2}}}\right]^{\frac{1}{2}}$ (4c)	Aveston & Sillwood (1976); Rosen (1964)
low elongation plate	plates	friction	$\frac{\epsilon_{lu}E_h\alpha b}{\tau}$ (5a)	$\frac{6\gamma_l V_l \tau}{E_c E_h \alpha^2 b}$ ‡(5b)	τ found from experiment	Argon & Shack (1975)
low elongation plate	plates	elastic	$\frac{\epsilon_{lu}E_h\alpha b}{\tau_{max}}$ (6a)	$\frac{2\gamma_l V_l \tau_{max}}{\alpha^2 E_c E_h b}$ ‡(6b)	$\Delta\sigma_0\left[\frac{G_l E_c}{E_h E_l V_l (d/b)}\right]^{\frac{1}{2}}$ (6c)	Aveston & Kelly (1973, this paper); Garrett & Bailey (1977*b*)†

† Garrett & Bailey (1977*b*) give the identical theory with a reference to Cox (1952). However, in Cox's theory the shearing component carries no tensile load, which is the essence of the problem here.

‡ See figure 1 for definition of b.

to 0.63 of the tensile fracture stress of the low elongation plate (90° lamella in this case) and both the interface and the plate are expected to be able to withstand this.

Since the theory has considerable practical application to restraining cracking in laminates, whether hybrid or not, and to increasing the first cracking strain of very stiff fibres in hybrid composites, it is worth emphasizing some simple points which should be taken into account in design. We illustrate these with the formulae for a plate or laminate analogous to figure 1(*c*) including, but not restricted to, a 0°/90°/0° laminate. If $2d$ is the thickness of the low elongation phase and b that of the high elongation phase on either side, then the crack spacing lies between x and $2x$, where x is given by

$$x = -\left[\frac{E_h E_l b d^2}{G_l E_c (b+d)}\right]^{\frac{1}{2}} \ln\left[1 - \frac{\epsilon_{lu} E_c}{\sigma_a}\right], \tag{4}$$

which reduces to equation (6*a*) in the table, by using equation (3), for σ_a greater than a few times $\epsilon_{lu} E_c$. If the two phases have not debonded from one another the value of τ_{max} can be deduced from formula (6*c*) of table 1. If debonding has occurred, which is probable if $\tau_{max} \gg \sigma_{lu}$, τ_{max} is due to sliding friction between the two components and this varies from 20 MN m^{-2} (Cooper & Sillwood 1972) for composites with a resin matrix to a few MN m^{-2} for composites with a cement matrix. In either case thinner lamellae mean more cracks per unit length. The maximum opening of each crack is

$$B \approx \epsilon_{lu}(1+\alpha)\, x, \tag{5}$$

so that the crack opening decreases with x and hence inversely as τ or τ_{max}. Thinner lamellae of the l.e. phase mean smaller openings to the cracks.

If crack openings are to be minimized then the two components and the interface between them must be able to withstand the value of τ_{max} given in the table without failure, i.e. the shear strength of the interface and components must be large. τ_{max} is given by

$$\tau_{max} = \epsilon_{lu} E_l \left\{\frac{E_c G_l}{E_h E_l}\left(1 + \frac{V_h}{V_l}\right)\right\}^{\frac{1}{2}}, \tag{6}$$

and hence increases with increase in the cracking strain of the l.e. phase. It may be desired to increase the cracking strain of the l.e. phase by reducing its dimensions so that the first cracking is constrained and the value of the cracking strain increased above that found in the same component outside the composite. Provided the value of τ_{max} in table 1 does not lead to interfacial failure so that the components remain elastically bonded, then the cracking strain of the l.e. lamellae varies inversely as the square root of the thickness, being given by

$$\epsilon_{lu} = \left\{\frac{2\gamma_l V_l}{E_c \alpha}\left(\frac{E_c G_l}{E_h E_l}\right)^{\frac{1}{2}} V_h^{-\frac{1}{2}} d^{-1}\right\}^{\frac{1}{2}}, \tag{7}$$

which is equivalent to equation (6*b*) in the table.

However, if the ability to constrain the cracking is governed by the highest value attainable for the shear stress between the cracked and uncracked components, then the maximum value of the cracking strain which can be attained is given by formula (5*b*) in the table and so ϵ_{lu} varies more slowly with decrease in the thickness of the l.e. phase. When elastic coherence between the two components breaks down, τ_{max} is replaced by τ, the sliding friction at the interface, and the constant 6 replaces 2 since additional (frictional) work has to be done by the applied stress when cracking occurs (Aveston & Kelly 1973). So far we have dealt with multiple cracking produced by an external stress applied to a composite. It can of course also arise from any form of internal straining, such as that due to a temperature change, and to control cracking of a

PHILOSOPHICAL TRANSACTIONS OF THE ROYAL SOCIETY A MATHEMATICAL, PHYSICAL & ENGINEERING SCIENCES

low elongation phase it must be shown that strains due to the various distortions, internal and external, are additive.

2.2. *Differential thermal stresses*

A laminate is normally cured above its service temperature so that considerable strains may exist in the lamellae as a result of differential thermal contraction between the plies. The problem is particularly acute with cross-ply laminates containing carbon fibre on account of its highly anisotropic thermal properties (see table 3). Each ply in a laminate is usually in tension normal to the fibres and since the failure strain in this direction is usually small there is a danger that advanced carbon fibre composites may be cracked even before they enter service. We have shown (Aveston *et al.* 1971) that the relation between cracking strain and the dimension of the l.e. phase is identical under external load and due to thermal loading so the same theory can be applied.

The constrained thermal strain in each component is given by

$$\epsilon_{\mathrm{l}}^{\circ} = \frac{\Delta T E_{\mathrm{h}} V_{\mathrm{h}}}{E_{\mathrm{c}}} (\alpha_{\mathrm{l}} - \alpha_{\mathrm{h}}) \tag{8}$$

and

$$\epsilon_{\mathrm{h}}^{\circ} = \frac{\Delta T E_{\mathrm{l}} V_{\mathrm{l}}}{E_{\mathrm{c}}} (\alpha_{\mathrm{h}} - \alpha_{\mathrm{l}}), \tag{9}$$

where α is the thermal expansion coefficient and ΔT is the difference between the service temperature and that below which thermal stresses are 'frozen in'. These stresses are independent of fibre or laminate thickness. It should be possible to control the cracking by specifying the maximum ply thickness that will yield an uncracked laminate for a given ΔT. We test the theory and illustrate this effect in § 3.

2.3. *Differential Poisson stresses*

Consider the 0°/90°/0° laminate in figure 1 (*c*). It does not appear to have been pointed out in the literature that, because of the small tensile cracking strain normal to the fibres, the presence of the 90° fibres (parallel to x), will tend to promote longitudinal splitting of the 0° lamellae. An example of the phenomenon is illustrated in figure 4. As with thermal strains, the strains generated by this effect depend only on volume fraction, but whether these lead to cracking or not can be made to depend on the thickness of the lamellae by making the lamellae sufficiently thin.

To estimate the effect, let subscripts 1 and 2 refer to the directions in the individual lamellae parallel and at right angles to the fibres respectively and x and y to the principal stress directions of the total laminate (figure 5). We call ν_{12} the contraction along 2 when the laminate is extended along 1; i.e. it is the principal Poisson ratio. For the individual orthotropic lamellae it is easily shown that

$$E_{11}\nu_{21} = E_{22}\nu_{12}. \tag{10}$$

Referring to figure 5, stress equilibrium in the x direction yields

$$E_{22}\epsilon_x(0°)\, 2b + E_{11}\epsilon_x(90°)\, 2d = 0, \tag{11}$$

and strain compatibility in the x direction gives for a strain ϵ_y of the composites,

$$\epsilon_x(0°) - \epsilon_x(90°) = (\nu_{12} - \nu_{21})\, \epsilon_y, \tag{12}$$

and hence substituting into equation (11) we have

$$\epsilon_x(0°) = E_{11}\left(\frac{d}{d+b}\right)(\nu_{12} - \nu_{21})\, \epsilon_y \Big/ \left\{E_{22}\left(\frac{b}{d+b}\right) + E_{11}\left(\frac{d}{d+b}\right)\right\} = E_{11}\left(\frac{d}{d+b}\right)(\nu_{12} - \nu_{21})\, \epsilon_y \Big/ E_{\mathrm{c}\perp}, \tag{13}$$

where $E_{\mathrm{c}\perp}$ is the Young modulus along the x direction of the laminate.

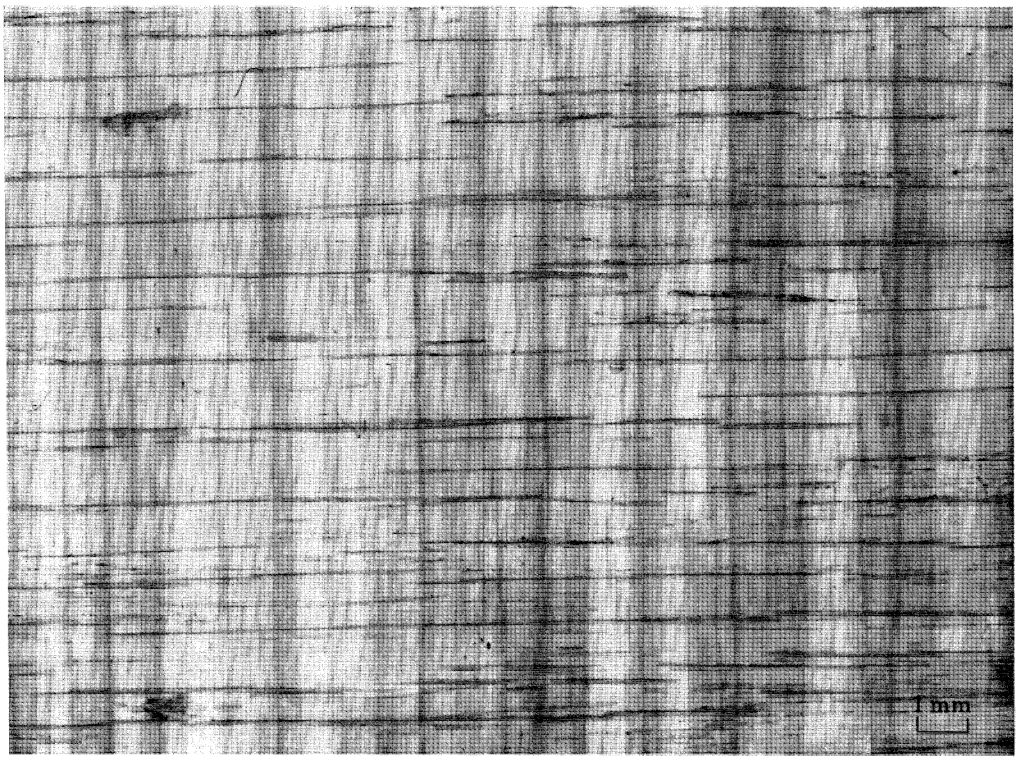

FIGURE 4. Transverse multiple cracking (vertical lines) and longitudinal splitting in glass–epoxy cross-ply laminate.

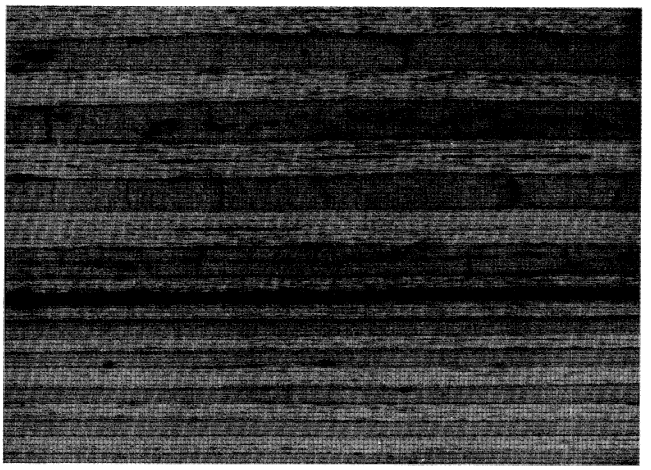

FIGURE 6. Sections through carbon–glass–epoxy laminates showing transverse thermal cracking in the 0.4 mm thick glass plies and crack suppression when the thickness is reduced to 0.2 mm.

(*Facing p.* 526)

PHILOSOPHICAL TRANSACTIONS OF THE ROYAL SOCIETY A MATHEMATICAL, PHYSICAL & ENGINEERING SCIENCES

In general E_{11} is much greater than E_{22} and therefore $\nu_{21} \ll \nu_{12}$. For example, for glass–polyester at $V_f = 0.3$, $\nu_{12} = 0.3$, $E_{11} = 25\ \mathrm{GN\,m^{-2}}$ and $E_{22} = 4\ \mathrm{GN\,m^{-2}}$ so that $(\nu_{12} - \nu_{21}) \approx 0.25$. If $b = d$ then $\epsilon_x(0°) \approx 0.22\epsilon_y$, so that in the absence of constraint effects we would expect to observe longitudinal splitting at a total laminate strain of some 4 or 5 times the first cracking strain. This is in fact observed in the experiments of Garrett & Bailey (1977*a*) who observed longitudinal cracks in the outer plies of a polyester–glass laminate made up as in figure 1(*c*), the individual plies of which had failure strain normal to the fibres of about 0.2 %. Its occurrence is now

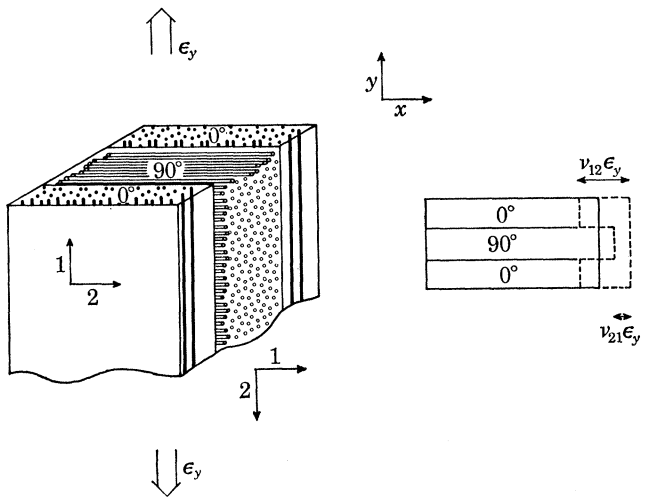

FIGURE 5. The origin of differential Poisson strains in a cross-ply laminate.

becoming well known and recognized. It may obviously occur in all laminates whether hybrid or not, and may be controlled either by arranging for an increase in the tensile failure strain measured normal to the fibres or else, if this cannot be done, by making the 0° layer thin enough to restrain cracking according to the theory reviewed in § 2.1. Again it must be borne in mind that differential thermal expansion effects will usually place the 0° layer in a laminate under transverse tension and so make it crack at a lower total additional strain than expected due to the differential Poisson effect. Bailey *et al.* (1979) are investigating some of these effects.

Actually, the estimate of strain parallel to x induced in the 0° plies by stretching the composite along y given by equation (13) will be an underestimate because, unless the transverse failure strain of the 0° plies is much less than that of the 90° plies, the latter will always crack first. The strain in the 90° layer will then be reduced, becoming zero at the crack, and the longitudinal strain in the 0° plies will be increased where they bridge the crack to a value $\epsilon_y(1+\alpha)$, so that the maximum transverse strain in the 0° layers is

$$\epsilon_x(0°) = \nu_{12}(1+\alpha)\,\epsilon_y, \tag{14}$$

and the mean strain will lie between $\nu_{12}(1+\frac{1}{2}\alpha)\,\epsilon_y$ and $\nu_{12}(1+\frac{3}{4}\alpha)\,\epsilon_y$, depending on whether the crack spacing is $2x$ or x. Thus if α is greater than about 2 we expect longitudinal splitting to be initiated by the transverse cracking in the absence of constraint, and with α greater than about 3, to be completed at the completion of transverse cracking. For given relative amounts of the 0° and 90° plies, reduction in the thickness of one of course automatically results in a reduction in the thickness of the other, so that longitudinal splitting may be reduced both on account of the increased transverse failure strain of the longitudinal plies and by the suppression of the initiating cracks in the 90° layers.

The glass–epoxy specimen shown in figure 4 (stress–strain curve, figure 2(*d*) and lamellae properties, table 3) consisted of ten 90° lamellae sandwiched between two outer 0° lamellae, so that from equation (14) $\epsilon_x(0°) = 0.9\epsilon_y$. From equations (8) and (9), the maximum thermal tensile strains in the 0° and 90° layers are 0.28 % and 0.11 % respectively, and from equation (7) the corresponding constrained cracking strains are 0.46 % and 0.16 %, compared with the normal transverse cracking strain of 0.22 %. We therefore expect transverse splitting to begin at a strain of (0.46–0.28)/0.9 = 0.2 %, and to be complete at the limit of multiple fracture. This was in fact observed; at the beginning of multiple cracking, small cracks were formed at right angles to the transverse cracks and by the completion of multiple cracking these had joined to form the pattern shown in figure 4.

2.4. *Impact*

It is an unfortunate fact that the stiffest composites have the lowest impact resistance. The reason, roughly speaking, is that the total strain energy of a composite at its u.t.s. is largely that of the fibres and for a given fibre strength this is inversely proportional to the fibre modulus. The same conclusion is reached if one considers that the work of fracture or toughness is governed by the contribution of the fibre strain energy over a 'debonded' region either side of a crack. In this case, of course, a larger debonded region (produced by a weak interface) will always improve the impact resistance compared with a shorter debonded length. As one of the main reasons for making a hybrid, apart from economy, is to improve the impact resistance of high modulus composites, it is of interest to compare the total energy per unit volume absorbed by a hybrid up to its u.t.s. with the sum of its components. Consider the idealized stress–strain curve in figure 3(*b*), appropriate to a mean crack separation of $\frac{3}{2}x$ so that the strain at the limit of multiple cracking becomes $\epsilon_{\mathrm{lu}}(1+\frac{5}{8}\alpha)$ and the ultimate failure strain $\epsilon_{\mathrm{hu}}-\frac{3}{8}\alpha\epsilon_{\mathrm{lu}}$, then the area *OABCD* is equal to

$$U_{\mathrm{a}} = \tfrac{1}{8}\alpha E_{\mathrm{c}}\epsilon_{\mathrm{lu}}^2 + \tfrac{1}{2}\epsilon_{\mathrm{hu}}^2 E_{\mathrm{h}} V_{\mathrm{h}}. \tag{15}$$

If the components were uncoupled, however, the stress–strain curve would follow the path *OAEF* and the energy absorbed to failure would be

$$U_{\mathrm{b}} = \tfrac{1}{2}E_{\mathrm{c}}\epsilon_{\mathrm{lu}}^2 + \tfrac{1}{2}E_{\mathrm{h}}V_{\mathrm{h}}\epsilon_{\mathrm{hu}}^2 - \tfrac{1}{2}E_{\mathrm{h}}V_{\mathrm{h}}\epsilon_{\mathrm{lu}}^2. \tag{16}$$

Subtracting (16) from (15) we find that the condition for the difference between the work of fracture of the coupled and uncoupled composite to be positive is that α be greater than 3. For example with the GRP–CFRP hybrid considered in § 3.2 there should be a synergistic toughening so long as the volume of carbon expressed as a fraction of the total volume is greater than 0.3. For multiple cracking to occur equation (2) must be obeyed, so in this case, taking $\epsilon_{\mathrm{hu}} = 2.3\,\%$ and $\epsilon_{\mathrm{lu}} = 0.28\,\%$ yields $\alpha > 7.1$ or a volume fraction of carbon of 0.48. Thus toughening is expected for volume fractions between 0.3 and 0.48 in this system. The overriding proviso in practice is that the required stiffness E_{c} can still be obtained when the stiffer fibres are diluted with high elongation fibres but cannot be obtained by using high strain fibres alone. The same stiffness could of course be obtained by using a lower volume fraction of the stiff fibres, but this is unlikely to be a practical solution as the energy under the stress–strain curve would be reduced to the small value OAH.

2.5. *Ultimate failure stress and strain*

Provided that the failure of the l.e. component provides no concentration of stress on the h.e. component, then when multiple fracture occurs the ultimate failure stress should be that of the

PHILOSOPHICAL TRANSACTIONS OF THE ROYAL SOCIETY A MATHEMATICAL, PHYSICAL & ENGINEERING SCIENCES

h.e. component multiplied by its volume fraction. The strain will be less, however, because the h.e. component is not stretched uniformly along its length and so, depending on whether the crack spacing is x or $2x$, the ultimate tensile strain of the composite ϵ_{cu} should lie between the limits

$$(\epsilon_{hu} - \tfrac{1}{2}\alpha\epsilon_{lu}) \leqslant \epsilon_{cu} \leqslant (\epsilon_{hu} - \tfrac{1}{4}\alpha\epsilon_{lu}) \tag{17}$$

(Aveston *et al.* 1971). Since this result is independent of the value of x it should be independent of whether or not the two phases are elastically bonded or debonded provided that in the elastically bonded case cracking has been carried to completion, i.e. an asymptotic value of crack spacing has been reached as a function of increasing composite strain (or applied stress), see § 2.1, equation (4).

The above simple theory for the longitudinal strength of a hybrid composite deals essentially with the effect on longitudinal strength of a composite, consisting of one set of aligned fibres in a resin matrix, of replacement of some of these fibres by others of differing elastic modulus and strength. The values of σ_{lu} and σ_{hu} are experimentally determined.

A more ambitious theory would attempt to account for the strength of a hybrid in terms of the properties of the individual fibres and of the resin. Such a theory would predict values of σ_{lu} and σ_{hu} as special cases. Zweben (1977) has attempted such a theory but gives an explicit result only for a 50:50 hybrid. Zweben's theory is based on the ideas of Rosen and Zweben (see Zweben 1972 for a summary), which have been successfully applied to predicting and explaining the strength of composites consisting of boron fibres in an aluminium matrix. Bounds are given for the strength. Summarized briefly, a lower bound for the strength is obtained by identifying the u.t.s. with that stress at which the first fibre fails. An upper bound treats the composite as a bundle of fibres of length equal to the ineffective length (transfer length) and lying between these two is the *fibre break propagation mode* in which the upper limit is reduced to take account of stress concentration on neighbouring fibres due to failure of a single fibre. We have modified bundle theory so that it applies to hybrid bundles and will report this work elsewhere.

3. Comparison with experiment

3.1. *Multiple cracking*

Much of the theory on multiple cracking and crack suppression has been tested by the group at N.P.L. over the past few years (Cooper & Sillwood 1972; Aveston *et al.* 1974; Aveston & Sillwood 1976). Other workers in widely varying fields have also reported experiments that are at least in qualitative agreement with the theory although a quantitative test is sometimes difficult on account of uncertainties in some of the parameters, particularly γ, and the difficulty of an independent estimate of τ, in the elastically debonded case. Aveston & Sillwood (1976) applied the theory particularly to hybrids and succeeded in increasing the cracking strain of carbon fibres of high modulus. They were careful to avoid thermal effects by using a resin which cures at room temperature. The agreement with theory is good but there is some uncertainty over the value of γ.

The most detailed experimental application of the theory to laminates is probably that of Parvizi *et al.* (1978) who studied cracking in 0°/90°/0° glass–epoxy laminates and concluded 'the onset of constrained cracking and its complete suppression can be accounted for remarkably well using the theory of Aveston & Kelly for the fully elastic case'.

There is, however, some uncertainty in the agreement with theory due to their complete

neglect of thermal effects. Also, Parvizi & Bailey (1978) have corrected the earlier result of Garrett & Bailey (1977*b*) for the variation of crack spacing with applied stress, and point out that the results of Stevens & Lupton (1977) can be interpreted on the same basis. These results are all accounted for well by equation (4) of this paper but there is uncertainty in all cases about the effect of thermal strains, which are probably masked by the spread in value of ϵ_{1u} in equation (4). Bader & Manders (1978) report that the failure strain of glass–carbon–epoxy hybrids increases as the thickness of the carbon plies decreases which is in accord with the theory. Laws (1974) found the cracking strain of glass fibre cement to increase with increasing volume fraction of glass fibres roughly in line with our theory. Finally in a different field Rabinovitch (1976) and Stoloff (1978) show that the yield point of directionally solidified eutectics, associated with

TABLE 2

lay-up, 3-ply	number of lamellae per ply: carbon	glass	carbon	calculated thermal strain in glass (90°) ply	predicted constrained cracking strain	crack spacing/mm
	5	10	5	0.0038	0.0020	4.4
	3	15	3	0.0035	0.0018	5.9
	2	20	2	0.0029	0.0016	6.5
	1	20	1	0.0023	0.0013	18
	1	26	1	0.0020	0.0011	uncracked
multiple ply cggcc...ggc, 10 carbon and 10 glass				0.0038	0.0045	1.1
multiple ply cgcg...gc, 6 carbon and 5 glass				0.0038†	0.0064	uncracked

† Tensile cracking strain found to be 0.0017 giving total 0.0055 – see text.

TABLE 3

property	carbon plies	glass plies
transverse failure strain	0.0047	0.0022
transverse modulus/(GN m^{-2})	6.9	15.7 GN/m^2
longitudinal modulus/(GN m^{-2})	198	48.6 GN/m^2
transverse expansion coefficient/K^{-1}	40×10^{-6}	24.1×10^{-6}
longitudinal expansion coefficient/K^{-1}	-0.7×10^{-6}	6.3×10^{-6}
surface work of fracture/(J m^{-2})	—	60
ply thickness per lamella/mm	0.20	0.20
transverse shear modulus/(GN m^{-2})	—	5 (assumed)
Poisson's ratio ν_{12}	0.30	0.33
Poisson's ration ν_{21}	0.01	0.11

multiple cracking of the more brittle fibre phase, increases as the diameter of the fibre decreases. This could have application to increasing the cracking strain of a brittle superconducting wire in a ductile normal conducting material.

3.2. *Thermal cracking*

Various 3-ply (as in figure 1(*c*)) and multiple-ply hybrids were prepared by hot pressing 'pre-preg' sheets of E-glass (90°) and surface treated type 1 carbon (0°) in a leaky mould with stops to give a finished thickness of 0.20 mm per lamella of pre-preg corresponding to an overall V_f of 0.62. The resin was Shell DX210 cured at 188 °C and cooled to ambient to give a maximum possible ΔT (equations 8 and 9) of 165°. The lay-ups are shown in table 2. The properties of the 100 % carbon and 100 % glass composites were measured and used to compute the restrained thermal shrinkages and constrained cracking strains in the transverse plies. The measured properties are given in table 3.

Referring to table 2 it is seen that for the 3-ply hybrids containing a relatively thick glass central layer the predicted constrained (elastic) cracking strain which would be obtained is always less than the observed unrestrained transverse failure strain and so we expect cracking as soon as the thermal strain exceeds the observed transverse failure strain of the glass ply – i.e. 0.22 % (table 3). This is in fact observed and indicates that our value of ΔT of 165 °C used to calculate the thermal strain cannot be greatly in error. For the two more highly dispersed multiple ply laminates the thermal strain is greater than the normal transverse failure cracking strain but the calculated constrained cracking strain is higher than both and so we should expect these to be uncracked. This prediction is only partially fulfilled, since the hybrid containing two lamellae per ply was in fact cracked. However, it should be noted that the predicted value of strain to be reached for cracking to occur (0.45 %) is only a little greater than the calculated value of the imposed thermal strain (0.38 %). On the other hand the hybrid containing individual lamellae remained uncracked, and in a subsequent tensile test cracked at a mechanically imposed strain of 0.0017 to give a total cracking strain for the 90° glass plies of 0.0056 compared with 0.0064 which is predicted. Figure 6 shows the two hybrids and the startling transition from cracked to uncracked on increasing the dispersion at approximately constant thermal strain.

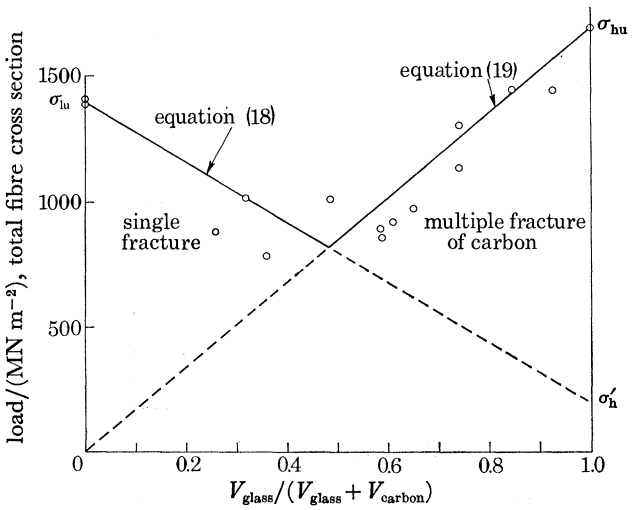

FIGURE 7. Tensile strength of aligned carbon–glass–epoxy hybrids plotted against glass content expressed as a fraction of the total fibre volume; σ_{hu} is the u.t.s. of the glass fibres and σ_{lu} that of the carbon.

3.2. *Ultimate failure stress and strain*

A range of glass–carbon–epoxy hybrids was prepared by impregnating tows of E-glass and Celanese GY70 carbon fibre with Araldite MY750-HY951 resin system and combining the impregnated strands to form an aligned intermingled hybrid bundle. The cross section of the component glass and carbon strands was obtained from the known densities and measured weight per unit length to give values of 5.84×10^{-4} and 2.08×10^{-4} cm² respectively. The hybrid bundles were cured *at room temperature* to avoid thermal effects, and the ends then encapsulated in special holders to facilitate alignment in the test machine.

Kalnin (1972) studied the failure stress of interlaminated carbon glass hybrids. His results for specimens stretched parallel to the fibres are quite consistent with the picture we now give, provided first cracking strain and ultimate failure are clearly distinguished. Figure 7 shows the variation of u.t.s. with glass content expressed as the fraction of the total fibre cross section (i.e.

ignoring the resin so that stresses are derived from the load by dividing by the known cross sectional area of the fibres). The addition of small quantities of glass fibre to the all-carbon fibre composite will lead to a decrease in strength since insufficient has been added to enable it to carry the load when the carbon breaks. Under these conditions, failure of the carbon leads to failure of the composite and there is no multiple fracture. The u.t.s. is given by

$$\sigma_{cu} = \sigma_{car,u} V_{car} + \epsilon_{car,u} E_g V_g, \tag{18}$$

where V_{car} and V_g are the fractions of the total fibre cross-section occupied by carbon and glass respectively. $\epsilon_{car,u}$ is the failure strain of the carbon in the hybrid. The line corresponding to equation (18) is plotted on figure 7. As V_g increases a transition occurs when there is sufficient glass to bear the total load when the carbon breaks. At volume loadings of glass above that of the transition the u.t.s. of the composite is given by

$$\sigma_{cu} = \sigma_{gu} V_g, \tag{19}$$

and it is seen from figure 7 that the experimental points remain close to this line. We deduce that in this particular experimental system the fracture of the carbon-containing strands does not produce a large stress concentration leading to weakening of the glass-containing strands.

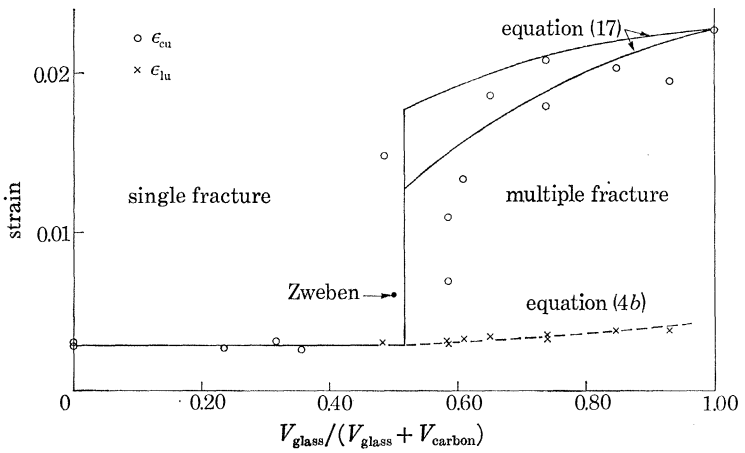

FIGURE 8. Ultimate failure strain (circles) and first cracking strain (crosses in the multiple cracking region) of aligned carbon–glass–epoxy hybrids.

The variation of ultimate tensile strain with fraction of glass in the reinforcement is shown in figure 8. At small volume fractions of glass the failure strain is that of the carbon and so ϵ_{cu} (marked by circles) is independent of composition and there is no multiple fracture. At a value of the transition point close to that given by equation (2) there is a sudden increase in ultimate failure strain to values that are close to the bounds given by equation (17), although slightly lower, as stress concentrations are not entirely absent. At the same time there is a small increase in ϵ_{lu} consistent with equation (4*b*) of table 1 (normalized to fit at $V_g = 0.5$ so as to avoid choosing a value for γ carbon). The transition point in terms of stress predicted from the experimental values of σ_{lu}, σ_{hu} and σ'_h differs slightly from the one in terms of strain plotted in figure 8 because we have ignored the small contribution of the resin to the total load. Also plotted in figure 8 is Zweben's (1977) prediction for the failure strain of a 50:50 hybrid, with his value of 10 for the Weibull parameters for both glass and carbon. The agreement is unlikely to be of significance

because the transition from single to multiple cracking occurs at 50 % volume fraction in these experiments where ϵ_{cu} is found to change by a large amount discontinuously.

Figure 9 shows the area under the stress–strain curve (i.e. total energy to failure per unit volume of glass plus carbon) as a function of V_g compared with the values predicted by equation (15). Again, there is a marked transition as the failure mode changes from single to multiple fracture. This plot emphasizes again that if h.e. fibres are added to increase toughness, the critical volume fraction must be exceeded so that single fracture is replaced by multiple fracture.

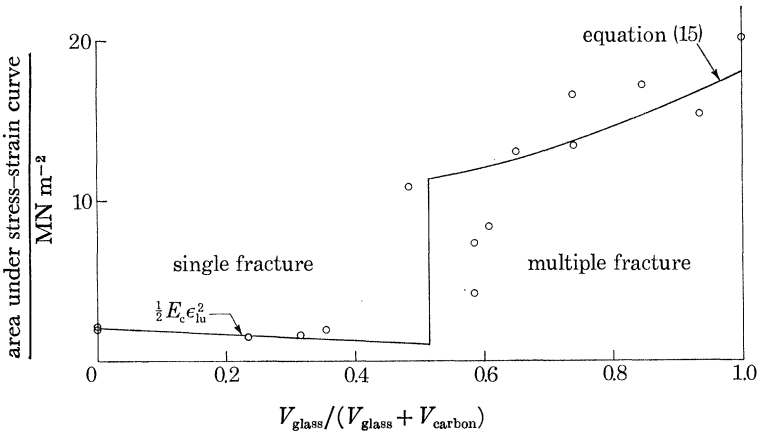

FIGURE 9. Total work of fracture as a function of glass content corresponding to the strengths and failure strains shown in figures 7 and 8.

We are very grateful to Mr J. Sillwood for help with the experiments and to Dr C. Zweben and Dr I. L. Kalnin for correspondence. Mr M. Bader, Mr P. W. Manders, Professor J. E. Bailey, Dr P. T. Curtis and Dr A. Parvizi kindly told us of their results before publication. We are grateful to the Director, National Physical Laboratory, for allowing this continuing cooperation between us.

REFERENCES (Aveston & Kelly)

Argon, A. S. & Shack, W. J. 1975 *Rilem Symposium Fibre Reinforced Cement and Concrete*, pp. 39–53. Construction Press, Ltd.

Aveston, J., Cooper, G. A. & Kelly, A. 1971 *Conference proceedings National Physical Laboratory: The properties of fibre composites*, pp. 15–26. I.P.C. Science and Technology Press, Ltd.

Aveston, J. & Kelly, A. 1973 *J. Mater. Sci.* **8**, 352–362.

Aveston, J., Mercer, R. A. & Sillwood, J. M. 1974 *Conference proceedings National Physical Laboratory: Composites – standards testing and design*, pp. 93–103. I.P.C. Science and Technology Press, Ltd.

Aveston, J. & Sillwood, J. M. 1976 *J. Mater. Sci.* **11**, 1877—1883.

Bader, M. G. & Manders, P. W. 1978 *Proceedings of the second international conference on composite materials*. Toronto, A.I.M.E.

Bailey, J. E., Curtis, P. T. & Parvizi, A. 1979 *Phil. Trans. R. Soc. Lond.* A **366**, 599–623.

Bibring, H., Rabinovitch, M. & Khan, T. 1972 *C. r. hebd. Séanc. Acad. Sci., Paris* **257**c, 1475–1478.

Bradley, P. D. & Harris, S. J. 1977 *J. Mater. Sci.* **12**, 2401–2410.

Bunsell, A. R. & Harris, B. 1974 *Composites* **5**, 157–164.

Cooper, G. A. & Sillwood, J. M. 1972 *J. Mater. Sci.* **7**, 325–333.

Cox, H. L. 1952 *Br. J. appl. Phys.* **3**, 72–79.

Durelli, A. J. & Okubo, S. 1953 *Proc. Soc. exp. Stress Analysis* **11**, 153–160.

Garrett, K. W. & Bailey, J. E. 1977*a* *J. Mater. Sci.* **12**, 2189–2194.

Garrett, K. W. & Bailey, J. E. 1977*b* *J. Mater. Sci.* **12**, 157–168.

Hancox, N. L. & Wells, H. 1974 *Proc. 2nd International Carbon Fibres Conference*, pp. 157–160. London: The Plastics Institute.

Harris, S. J. & Bradley, P. D. 1976 *International conference on composite materials*, vol. 1, pp. 327–335. Geneva: A.I.M.E.
Harris, B. & Bunsell, A. R. 1975 *Composites* **6**, 197–201.
Kalnin, I. L. 1972 *Composite Materials Testing and Design*, ASTM STP 497, pp. 551–563.
Kelly, A. 1974 *Conference proceedings National Physical Laboratory: Composites – standards testing and design*, pp. 9–15. I.P.C. Science and Technology Press, Ltd.
Kelly, A. 1976 In *Frontiers in materials science* (ed. L. E. Murr & C. Stein), pp. 335–364. New York: Marcel Dekker Inc.
Kelly, A. 1978 In *Advances in composite materials* (ed. G. Piatti), pp. 113–129. London: Applied Science Publishers Ltd.
Laws, V. 1974 *Conference proceedings National Physical Laboratory: Composites – standards testing and design*, pp. 102, 103.
Lekhnitskii, S. G. 1968 *Anisotropic plates*. London: Gordon and Breach.
Lovell, D. R. 1974 *Proc. 2nd International Carbon Fibres Conference*, pp. 283–289. London: The Plastics Institute.
Owen, M. J. 1974 *Composite materials*, vol. v, pp. 342–368. New York: Academic Press.
Parvizi, A. & Bailey, J. E. 1978 *J. Mater. Sci.* **13**, 2131–2136.
Parvizi, A., Garrett, K. W. & Bailey, J. E. 1978 *J. Mater. Sci.* **13**, 195–201.
Paton, W. 1977 *National Engineering Laboratory Report* no. 633. *Reinforced plastics laminates of hybrid construction.*
Rabinovitch, M. 1976 *Advances in composite materials:* course at I.S.P.R.A., Italy.
Romualdi, J. P. & Batson, G. B. 1963 *Proc. Am. Soc. civ. Engrs* **84**, 147–168.
Sendeckyj, G. P. 1974 *Composite materials*, vol. II, pp. 46–82. New York: Academic Press.
Spurrier, J. & Luxmore, A. R. 1976 *Fibre Sci Tech*, no. 1, **9**, 225.
Stevens, G. T. & Lupton, A. W. 1977 *J. Mater. Sci.* **12**, 1706–1708.
Stoloff, N. S. 1978 In *Advances in composite materials* (ed. G. Piatti), pp. 247–285. London: Applied Science Publishers Ltd.
Tardiff, G. Jr 1973 *Engng Fract. Mech.* **5**, 1–10.
Walton, P. L. & Majumdar, A. J. 1975 *Composites* **6**, 209–216.
Zweben, C. 1972 *Engng Fract. Mech.* **4**, 1–7.
Zweben, C. 1977 *J. Mater. Sci.* **12**, 1325–1337.

PHILOSOPHICAL TRANSACTIONS OF THE ROYAL SOCIETY A MATHEMATICAL, PHYSICAL & ENGINEERING SCIENCES

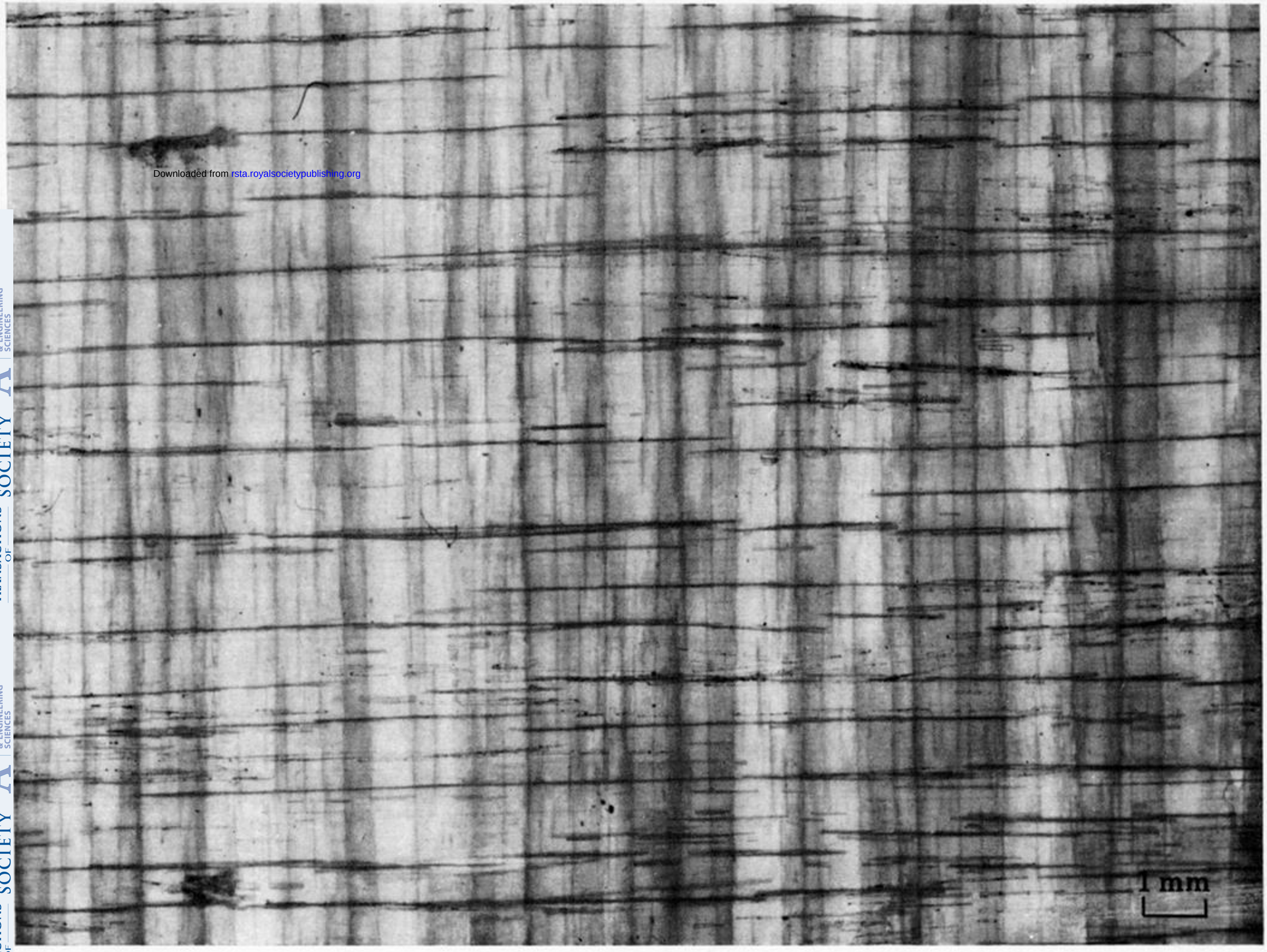

FIGURE 4. Transverse multiple cracking (vertical lines) and longitudinal splitting in glass–epoxy cross-ply laminate.

PHILOSOPHICAL TRANSACTIONS OF THE ROYAL SOCIETY A MATHEMATICAL, PHYSICAL & ENGINEERING SCIENCES

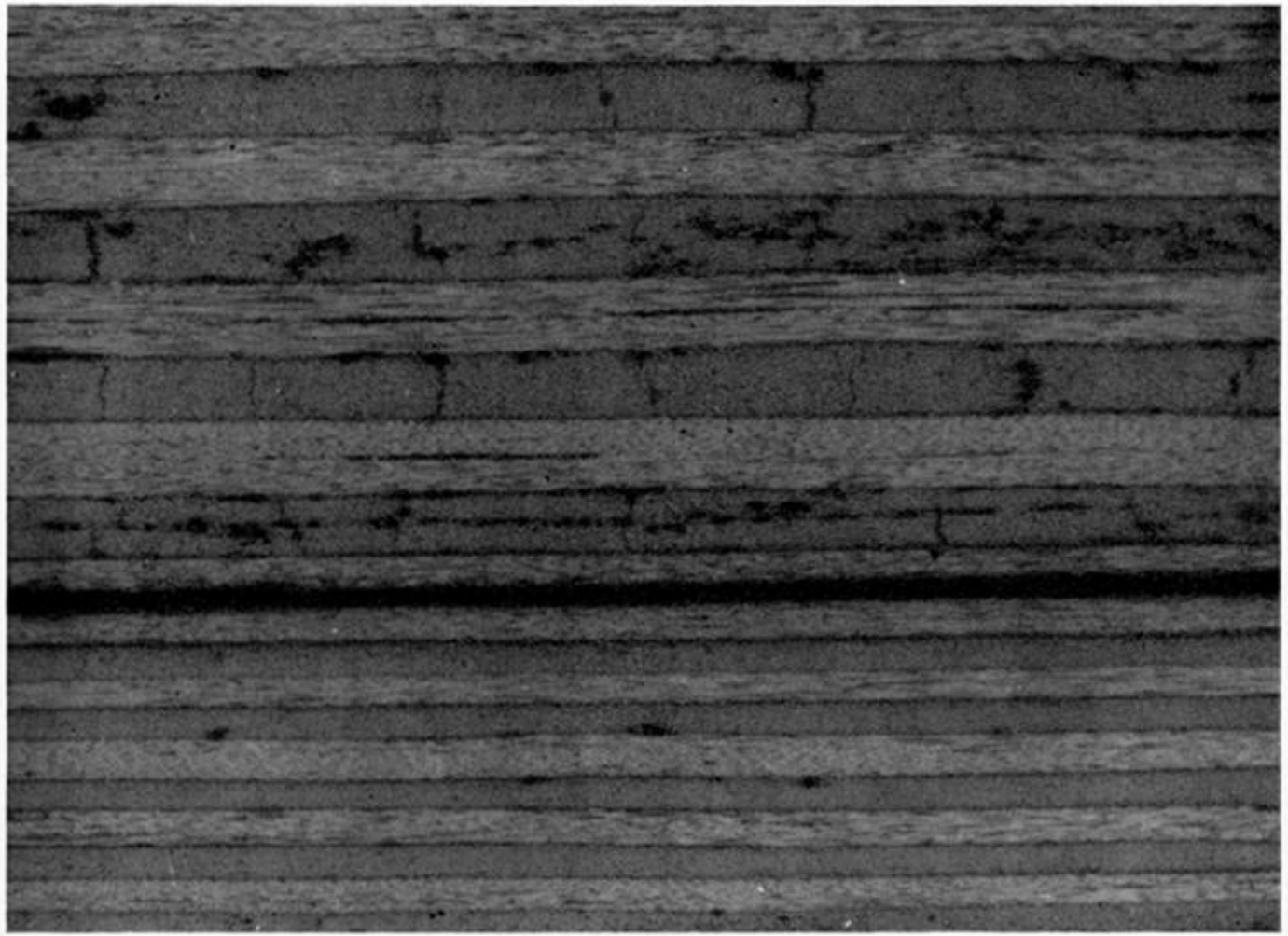

FIGURE 6. Sections through carbon–glass–epoxy laminates showing transverse thermal cracking in the 0.4 mm thick glass plies and crack suppression when the thickness is reduced to 0.2 mm.

PHILOSOPHICAL TRANSACTIONS OF THE ROYAL SOCIETY A MATHEMATICAL, PHYSICAL & ENGINEERING SCIENCES